Dalton Transactions

An international journal of inorganic chemistry

Accepted Manuscript

This article can be cited before page numbers have been issued, to do this please use: A. I. B. Romo, M. S. Carepo, P. Levin, O. Nascimento, D. E. Diaz, J. Rodriguez-Lopez, I. E. León, L. F. Bezerra, L. A. Lemus and I. C. N. DIOGENES, *Dalton Trans.*, 2021, DOI: 10.1039/D1DT01358K.

ROYAL SOCIETY OF CHEMISTRY

rsc.li/dalton

View Article Online
DOI: 10.1039/D1DT01358K

Synergy of DNA intercalation and catalytic activity of a copper complex towards improved polymerase inhibition and cancer cell cytotoxicity

Received 00th January 20xx,
Accepted 00th January 20xx

DOI: 10.1039/x0xx00000x

Adolfo I. B. Romo*[ab], Marta P. Carepo,[c] Pedro Levín,[d] Otaciro R. Nascimento,[e] Daniel E. Díaz, [d] Joaquín Rodríguez-López,[b] Ignácio E. León,[f] Lucas F. Bezerra,[a] Luis Lemus[d] and Izaura C. N. Diógenes*[a]

Improving the binding of metal complexes to DNA to boost cancer cell cytotoxicity requires fine tuning of their structural and chemical properties. Copper has been used as metal center in compounds containing intercalating ligands due to its ability to catalytically generate reactive oxygen species (ROS), such as hydroxyl radical (OH•). We envision the synergy of DNA binding and ROS generation at proximity from target DNA as a powerful chemotherapy treatment. Here, we explore the use of $[Cu(2CP\text{-}Bz\text{-}SMe)]^{2+}$ (2CP-Bz-SMe = 1,3-bis(1,10-phenanthrolin-2-yloxy)-N-(4-(methylthio)benzylidene)propan-2-amine) for this purpose by characterizing its cytotoxicity, DNA binding, and ability to affect DNA replication through polymerase chain reaction – PCR and nuclease assays. We determined binding (K_b) and Stern-Volmer constants (K_{SV}) for complex-DNA association of 5.8 ± 0.14 x10^4 and 1.64 (±0.08), respectively, through absorption titration and competitive fluorescence experiments. These values were superior to those of other Cu-complex intercalators. We hypothesize that the distorted trigonal bipyramidal geometry of $[Cu(2CP\text{-}Bz\text{-}SMe)]^{2+}$ allows the phenanthroline fragments to be better accommodated into the DNA double helix. Moreover, the aromaticity of these fragments increases the local hydrophobicity thus increasing the affinity for the hydrophobic domains of DNA. Nuclease assays in the presence of the common reducing agents ascorbic acid, nicotinamide adenine dinucleotide, and glutathione showed effective in degradation of DNA due to the in situ generation of OH•. The $[Cu(2CP\text{-}Bz\text{-}SMe)]^{2+}$ complex showed cytotoxicity against the following human cancer cells lines A549, MCF-7, MDA-MB-231 and MG-63 with half maximal inhibitory concentration (IC_{50}) values of 4.62 ± 0.48, 5.20 ± 0.76, 5.70 ± 0.42 and 2.88 ± 0.66 μM respectively. These low values of IC_{50}, which are promising if compared to cisplatin, are ascribed to the synergistic effect of ROS generation with the intercalation ability into the DNA minor grooves and blocking DNA replication. This study introduces new principles for synergizing chemical and structural properties of intercalation compounds for improved drug-DNA interactions targeting cancer.

Introduction

Research on cancer treatments have exhaustively focused on the search of compounds able to specifically interact with cancer cells without (or with minimum) side effects. Synthetic molecules have been developed to interrupt or modify the double-stranded replication of DNA via recognition and subsequent Drug-DNA interactions, which constitute the basis of current chemotherapy treatments, can occur in the major and/or minor grooves[1,2] through electrostatic and covalent bonds.[3] Such interactions may interrupt DNA replication and/or induce degradation if the drug constituents produce, for example, reactive oxygen species (ROS).[4-7] Copper has been used as metal center in compounds containing intercalating ligands aiming to produce ROS in proximity to the target. Pitié et al[8,9] reported nuclease activity of a series of copper compounds containing phenanthroline-derived ligands. In comparison to the copper complex containing two phenanthroline ligands, $[Cu(phen)_2]^+$, an improvement of about 60 times was observed when the metal was coordinated to clip-phen, which consists of two phenanthroline moieties tethered by an alkyl spacer at the C2 or C3 positions.[8,10,11] Such arrangement provides greater stability against ligand decordination since the geometry of copper compounds is dependent on the oxidation state, usually tetrahedral and square planar for Cu^I and Cu^{II}, respectively.[12,13] It should be noted here that the ROS generation by copper compounds is often related to Fenton-like reactions in which the metal center necessarily undergoes changes in the oxidation state. Indeed, the nuclease activity induced by copper complexes containing phen derivatives has been assigned to the deleterious effect of ROS, mainly hydroxyl radical (OH•), which

[a] Departamento de Química Orgânica e Inorgânica, Centro de Ciências, Universidade Federal do Ceará, Cx. Postal 6021, Fortaleza, CE, 60451-970, Brasil. E-mail: izaura@dqoi.ufc.br
[b] Department of Chemistry and Beckman Institute for Advanced Science and Technology, University of Illinois at Urbana–Champaign, Urbana, Illinois 61801, United States. E-mail: adolfo@illinois.edu
[c] LAQV, REQUIMTE, Departamento de Química, Faculdade de Ciências e Tecnologia, Universidade Nova de Lisboa, 2829-Caparica, Portugal.
[d] Facultad de Química y Biología, Universidad de Santiago de Chile. Alameda 3363, Estación Central, Santiago, Chile.
[e] Departamento de Física Interdiciplinar, Instituto de Física de São Carlos. Universidade de São Paulo, CP 369, CEP 13560-970 São Carlos, SP, Brazil.
[f] Centro de Química Inorgánica, (CONICET-UNLP) Bv. 120 e/ 60 y 64 Nº1465, La Plata, Argentina.

are produced through oxidative pathways following multiple steps that involves, at first, the reduction of Cu^{II} to Cu^{I} that is, in turn, oxidized back to Cu^{II} producing ROS if in aerated aqueous medium.[14-16] However, both the nature of the ROS and the mechanism have been focus of debate. While electron paramagnetic resonance (EPR) data point for $OH^{\bullet}$ as ROS,[14,17-19] UV-Vis spectra at low temperatures (T < -50 °C) strongly suggest the formation of a Cu^{II} binuclear intermediate having O_2^{-2} or ^{-}OOH as bridging ligand.[14,16,20-23] In addition, at mild conditions (room temperature), we had success in detecting a binuclear Cu^{I}-O_2-Cu^{I} intermediate through surface plasmon resonance (SPR) technique.[18] For this purpose, a thioether fragment was attached to clip-phen (2CP-Bz-SMe) making the compound susceptible to adsorb on gold which was further probed via surface-enhanced Raman scattering (SERS). The SPR experiments were performed by using gold chips modified with $[Cu(2CP\text{-}Bz\text{-}SMe)]^{2+}$ in an electrochemical cell with constant flow of electrolytic solutions, with and without the copper complex. Whenever a sufficiently negative potential to reduce to Cu^{I} was applied in the presence of the complex, there was an increase at the SPR angle consistent with the formation of a binuclear compound connected through an O-O bridge. Also, images of scanning electrochemical microscopy (SECM) and EPR data showed the $[Cu(2CP\text{-}Bz\text{-}SMe)]^{2+}$ complex is able to generate $OH^{\bullet}$ upon adsorption on gold electrode[18,24] and gold-coated magnetic nanoparticles.[17] In both cases, electrophoresis indicated DNA degradation thus making the $[Cu(2CP\text{-}Bz\text{-}SMe)]^{2+}$ complex a promising candidate for anticancer studies. Here, we further probe the interaction of this complex with DNA (PCR reactions, Stern-Volmer and binding constants) as well as its cytotoxicity against three human cancer cells lines (A549, MCF-7 and MDA-MB-231).

Experimental

Chemicals

All experiments used purified water from a Millipore Milli-Q Biocel system. Methanol and dimethylformamide, from Merck, were dried over 4 Å molecular sieves previously calcined. Acetonitrile, from Merck, was dried by refluxing over P_2O_5, from Sigma-Aldrich. Deuterated tetrachloroethane (d_2-TCE) was purchased from Sigma-Aldric and used as received. Copper precursor, $[Cu^{I}(CH_3CN)_4](ClO_4)$, was synthesized according to the literature.[19] DNA binding studies were performed using Calf-Thymus DNA (ct-DNA) and Ethidium Bromide (EB) from Sigma Aldrich. Ascorbic acid (AA), nicotinamide adenine dinucleotide (NADH), and glutathione (GSH) were purchased from Sigma Aldrich and used as received. Plasmid pBR322 was purchased from BioLabs. Buffer phosphate solution (PBS, pH 7.4) was prepared with Na_2HPO_4 and NaH_2PO_4 from Sigma Aldrich. TAE buffer pH 8.0 was prepared by mixing 40 mM buffer Tris (2-Amino-2-(hydroxymethyl)-1,3-propanediol), 1 mM EDTA, 20 mM acetic acid and agarose gel available in Sigma Aldrich. All polymerase chain reaction (PCR) reagents were purchased from NZYTech: buffer Tris-HCl (pH 8.8), $(NH_4)SO_4$, KCl, $MgSO_4$, Triton-100, dNTP mix, NZYProof DNA Polymerase and Oligonucleotide Ladder.

Apparatus

View Article Online
DOI: 10.1039/D1DT01358K

1D and 2D nuclear magnetic resonance (NMR) experiments were performed on a Bruker Avance-400 instrument operating at 400.13 MHz for ^{1}H and 100.61 MHz for ^{13}C nucleus respectively, equipped with a 5 mm multinuclear broad-band dual probehead (^{109}Ag–^{31}P), incorporating a z-gradient coil. The NMR spectra were calibrated in respect to $CDCl_3$ or d_2-TCE and corrected relative to tetramethylsilane (TMS). Typically 16 scans were used in each experiment. Electronic spectra in the ultraviolet and visible (UV-Vis) regions were acquired on an Analytik Jena Specord S-100 spectrophotometer at room temperature in a 1.0 cm quartz cell. Fluorescence studies were recorded using a PTI Quanta-Master QM-40 fluorescence spectrophotometer at room temperature in a 1.0 cm quartz cell. The ESR measurement were acquired at RT (298 K) with a EMXPlus X-band instrument using a Wilmad Flat cell and simulated with Easyspin program.[60]

Synthetic procedures

1,3-bis((1,10-phenanthrolin-2-yl)oxy)-N-(4-(methylthio)benzylidene) propan-2-imine, (2CP-Bz-SMe). The Lewis base 2CP-Bz-SMe was successfully prepared according to previously reported procedures[18] as indicated by the ^{1}H-NMR spectrum. ^{1}H-NMR (d_2-TCE): δ(ppm) = 9.16 (d, 2H), 8.64 (s, 1H), 8.27 (d, 2H), 8.15 (d, 2H), 7.78 (d, 2H), 7.77 (d, 2H), 7.70 (d, 2H), 7.63 (dd, 2H), 7.28 (d, 2H), 7.20 (d, 2H), 5.18 (m, 2H), 5.12 (m, 2H), 4.46 (q, 1H), 2.53 (s, 3H).

$[Cu^{II}(2CP\text{-}Bz\text{-}SMe)(NO_3)](NO_3)$. The cupric complex was prepared according to the reported procedure.[18] (ESI, positive mode) m/z: 322.05862 ($[Cu(2CP\text{-}Bz\text{-}SMe)]^{2+}$) = ($C_{35}H_{27}O_2N_5SCu^{2+}$).

DNA-binding studies

The affinity of $[Cu(2CP\text{-}Bz\text{-}SMe)]^{2+}$ towards DNA was evaluated by using Calf-thymus DNA (ct-DNA) in PBS (10 mM, pH 7.4). These studies were performed by titration (absorption spectroscopy) and competition displacement (emission spectroscopy) of ethidium bromide (EB) for determining the binding (K_b) and the Stern-Volmer (K_{SV}) constants, respectively. The absorbance at 260 nm and 280 nm of ct-DNA in PBS gave a ratio of 1.83 indicating ct- DNA is protein free.[25] The concentration of ct-DNA was calculated from its absorption at 260 nm, considering a molar extinction coefficient value of 6600 $M^{-1}cm^{-1}$.[26] Absorption titration experiments were performed by adding different concentrations of ct-DNA to a 2 x 10^{-5} M solution of $[Cu(2CP\text{-}Bz\text{-}SMe)]^{2+}$. The absorbance values were corrected for dilution and the value of K_b was obtained by Equation 1[27]:

$$\frac{[\mathbf{bp}]}{(\varepsilon_a-\varepsilon_f)} = \frac{[\mathbf{bp}]}{(\varepsilon_b-\varepsilon_f)} + \frac{\mathbf{1}}{\boldsymbol{K_b}(\varepsilon_b-\varepsilon_f)} \qquad \text{Eq. 1}$$

where [bp] is the concentration of ct-DNA in base pairs, ε_a is the apparent extinction coefficient at each DNA addition, ε_f and ε_b are the extinction coefficients of the free complex and the complex bounded to DNA, respectively.[28] The assays of competitive displacement of EB by $[Cu(2CP\text{-}Bz\text{-}SMe)]^{2+}$ were performed by adding aliquots of $[Cu(2CP\text{-}Bz\text{-}SMe)]^{2+}$ (from 0 to 1 μM) to a solution of 10 mM PBS containing 1 μM of EB and 10 μM of ct-DNA previously incubated for 24 h. Emission spectra were recorded in the range from 550 to 700 nm after irradiation at 495 nm, before and after the addition of the copper complex. Dilution

at final addition was lesser than 5%. The Stern-Volmer constant was extracted from Equation 2[29]:

$$\frac{I_0}{I} = 1 + K_{sv}[Q] \qquad \text{Eq. 2}$$

where I_0 and I are the fluorescence intensities at the beginning and upon consecutive additions of the complex whose concentration is included as [Q].

Cytotoxicity assays

In vitro cytotoxicity assays on cultured human tumor cell lines represent the standard method for initial screening of antitumor agents. Thus, as a first step to assess their pharmacological properties, $[Cu(2CP\text{-}Bz\text{-}SMe)]^{2+}$ was assayed against the following cells: triple breast negative human MDA-MB-231 (ATCC HTB-26), human lung adenocarcinoma A549 (ATCC CCL185), hormone dependent human breast MCF-7 (ATCC HTB-22) and bones fibroblast MG-63 (ATCC CRL-1427). The cells were routinely maintained following the ATCC (American Type Culture Collection) recommendations. To evaluate the growth inhibition, the cells were seeded in 96-well plates (Corning Costar) at a concentration of 2×10^4 cells/well and grown for 24 h in complete medium, i.e. Dulbecco's Modified Eagle Medium (DMEM) + 10% of Fetal Bovine Serum (FBS). Aliquots of 0.75 µL of the solutions of $[Cu^{II}(2CP\text{-}Bz\text{-}SMe)]^{2+}$, which were prepared by diluting a freshly prepared stock solution (20 mM in DMSO), were added to 150 µL of the culture medium. The percentage of DMSO in the medium never exceeded 0.5%; at this concentration, DMSO has no effect on the cell viability.[30] Afterward, the medium was changed and the cells were incubated with 0.5 mg/mL of 3-(4,5-dimethylthiazol-2-yl)-2,5-diphenyltetrazolium bromide (MTT) under normal culture conditions for 3 h. The MTT assay is based on the fact that only live cells reduce MTT to purple formazan products thus allowing the cell counting. After the incubation for 3h, the cell culture medium was removed and the purple formazan was dissolved in DMSO. The optical density of each well (96-well plates) was quantified at 540 nm using a multiwell plate reader and the percentage of surviving cells was calculated from the absorbance ratio of treated to untreated cells. The half maximal inhibitory concentration (IC_{50}) value was calculated as the concentration reducing the viability of the cells by 50% and is presented as a mean (±SE) of at least three independent experiments.

Plasmid pBR322 cleavage assays using different reducing agents

Cleavage assays of supercoiled plasmid pBR322 were acquired in 20 µL of 10 mM PBS (pH 7.4). In all assays, the concentrations of DNA and $[Cu(2CP\text{-}Bz\text{-}SMe)]^{2+}$ were kept constant at 5 ng/µL and 10 µM, respectively. Control runs were performed in PBS containing only the plasmid DNA in the same experimental conditions. Three reducing agents were tested in different concentrations, NADH (0.1 and 0.2 mM), GSH (1.5 and 4 mM) and ascorbic acid (0.1 mM). After incubation for 30 min, 4 µL of 6X DNA loading dye (Biolabs) were added to the reaction mixture and the samples were immediately loaded in a 0.8% agarose gel prepared in TAE buffer pH 8.0 (40 mM Tris, 20 mM acetic acid, 1 mM EDTA) and electrophoresed in a horizontal electrophoresis system (Bio-Rad) at 70 V. After electrophoresis, the gels were stained using SYBR Safe DNA gel stain (Invitrogen). Band intensities were calculated as a percentage of the intensity of the control band using the program ImageJ. It is worth mentioning that UV-Vis spectra of the complex in PBS were acquired (data not shown) upon addition of the reducing agents. These spectra showed the emergence of a band at c.a. 410 nm assigned to metal-to-ligand charge-transfer (MLCT) transitions typically seen in copper(I) compounds containing aromatic ligands.[24] This behavior indicates the complex is stable in the reducing media used in the cleavage assays experiments.

ESR measurements

ESR spectra were obtained at room temperature from aqueous non-deareated solution of the complex at final concentration 30 µM, witch were mixed with AA, GSH and NADH at final concentration of 50 µM containing the spin trap 5,5-Dimethyl-1-pyrroline-N-oxide (DMPO) at final concentration of 200 µM. Measurement condition: center field 3488 G, sweep field 100 G, sweep time 60 s, MW power 20 mW, gain 2.0×10^3, modulation amplitude 1 G, modulation frequency 100 kHz, time constant: 0.064 s, MW frequency: 9.796620 GHz.

PCR inhibition assays

All polymerase chain reaction (PCR) reagents were purchased from NZYTech. PCR reactions were performed in total volume of 20 µL: 20 mM Tris-HCl (pH 8.8), 10 mM $(NH_4)SO_4$, 10 mM KCl, 2 mM $MgSO_4$ and 0.1% Triton-100, 0.2 mM dNTP mix, 0,16 U of DNA polymerase (NZYProof DNA Polymerase), 0.2 µM primers forward and reverse and 14 ng of bacterial DNA template. A range from of 1 to 5 µM of the complex concentrations was added to the PCR mixtures. The PCR reactions were performed using the following parameters: initial denaturation step of 2 min at 95 ºC, followed by 30 cycles of denaturation for 1 min at 95 ºC, annealing at 60 ºC for 40 s and extension at 72 ºC for 80 s. An additional extension step was performed at 72 ºC for 10 min. The expected size of the amplicon is 1300 bp. A control reaction without the copper compound was performed. In addition, UV-Vis spectra of the complex were obtained in the PCR medium at different temperatures and showed no changes indicating the complex stability in the studied conditions (data not shown).

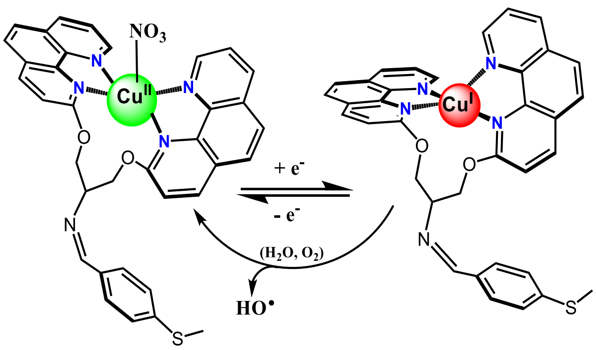

Figure 1. Depiction of the structural transformation of $[Cu(2CP\text{-}Bz\text{-}SMe)]^{2+}$ from distorted trigonal bipyramid to tetrahedral geometry; reoxidation of the complex in aerated aqueous medium generates $OH^{\bullet}$.

Results and discussion

As reported previously,[18] the EPR spectrum of $[Cu(2CP\text{-}Bz\text{-}SMe)]^{2+}$ indicates a distorted trigonal bipyramidal geometry

View Article Online
DOI: 10.1039/D1DT01358K

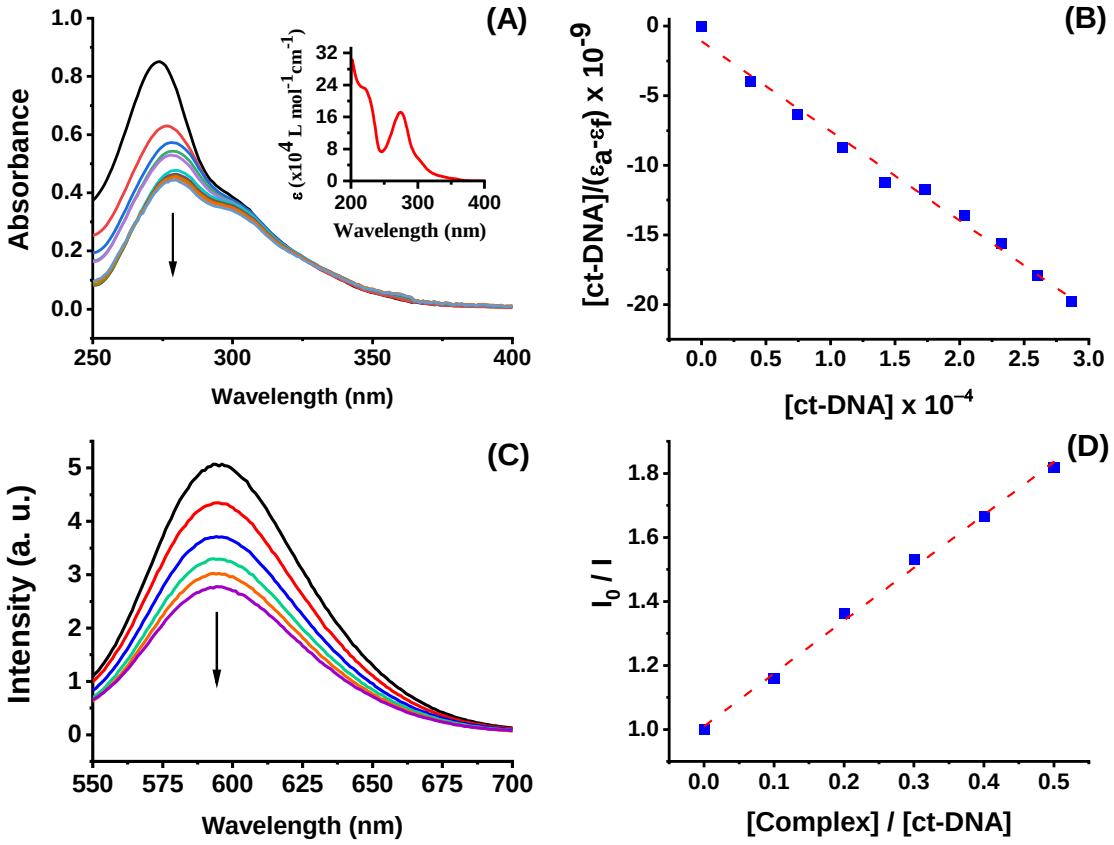

Figure 2. (A) Spectroscopic titration (absorption) of 2 x 10^{-5} M $[Cu(2CP\text{-}Bz\text{-}SMe)]^{2+}$ in 10 mM PBS with aliquots of 50 μL of 1.56 x 10^{-3} M ct-DNA in 10 mM PBS (pH 7.4). Inset: UV-Vis spectrum of $[Cu(2CP\text{-}Bz\text{-}SMe)]^{2+}$ in 10 mM PBS. **(B)** Plot of [ct-DNA]/(ε_a-ε_f) vs [ct-DNA]. **(C)** Spectroscopic titration (emission) of the DNA-EB adduct with aliquots of 20 μL of $[Cu(2CP\text{-}Bz\text{-}SMe)]^{2+}$ (2x10^{-5} M). **(D)** Plot I_0/I vs [Complex]/[ct-DNA].

with the 2CP-Bz-SMe ligand bonded to the copper center through the nitrogen atoms. If the antitumoral activity of $[Cu(2CP\text{-}Bz\text{-}SMe)]^{2+}$ is based on ROS generation,[4-7] its ligand structural arrangement in the coordination sphere should confer stability to withstand changes in the oxidation state of copper without bond breaking. It is worth mentioning that the $[Cu(2CP\text{-}Bz\text{-}SMe)]^{2+}$ complex presents a quasi-reversible redox behavior centred at 0.13 V vs Ag/AgCl, as determined by cyclic voltammetry,[18] indicating the easiness of the redox change. Fig. 1 depicts how the local symmetry around the copper ion is modified upon changes in the oxidation state of $[Cu(2CP\text{-}Bz\text{-}SMe)]^{2+}$ as it produces $OH^{\bullet}$ in aerated aqueous medium. Phenanthroline-like ligands not only stabilize different oxidation states of copper, but also facilitate intercalation in DNA, enhancing the proximity between the complex and the nucleic acid.11 In addition, as already reported,18 the ligand has a serinol bridge (-O-CH2-CH(N=R)-CH2-O-) that increase the degrees of freedom allowing it to adapt to geometric changes as consequence of the oxidation changes of copper required for radical production. We posited that the ability of 2CP-Bz-SMe to intercalate and to stabilize the Cu oxidation states required for $OH^{\bullet}$ generation near DNA enhances the cytotoxicity of $[Cu(2CP\text{-}Bz\text{-}SMe)]^{2+}$ towards the three types of human cancer cells studied.

DNA binding studies

The intrinsic binding constant (K_b) obtained by absorption titration is one of the most used parameters for quantifying the affinity of DNA with drugs [30-34]. The UV-Vis spectrum of $[Cu(2CP\text{-}Bz\text{-}SMe)]^{2+}$ in aqueous solution free of DNA (inset in Fig. 2, A) shows bands from 200 to 350 nm, assigned[35] to the intraligand transitions of 2CP-Bz-SMe, and 840 nm (not shown) ascribed[36] to the ligand field transitions. In order to quantitatively evaluate the interaction of $[Cu(2CP\text{-}Bz\text{-}SMe)]^{2+}$ with DNA, the behavior of the band at 274 nm was spectroscopically monitored upon successive additions of ct-DNA to a 2 x 10^{-5} M solution of the complex (Fig. 2, A). By using Equation 1, the slope-to-intercept ratio of the plot of [ct-DNA]/($\varepsilon_a - \varepsilon_f$) vs [ct-DNA] (Fig. 1, (B)) gave the value of K_b (5.8 ± 0.14 x10^4).

The additions of ct-DNA to the solution of $[Cu(2CP\text{-}Bz\text{-}SMe)]^{2+}$ resulted in hypochromism of the band at 274 nm, indicating intercalation or electrostatic interaction between the copper compound and DNA. This behavior along with the observed red shift indicates the compound interacts with DNA, in accordance with theoretical data that predict phenanthroline-like ligands

View Article Online
DOI: 10.1039/D1DT01358K

Table 1. Binding (K_b) and Stern-Volmer (K_{SV}) constants, and geometries of a few copper(II) complexes.

Complex	K_b ($x10^3$ M^{-1})	K_{SV}	Geometry	Ref.
$[Cu(2CP\text{-}Bz\text{-}SMe)]^{2+}$	50.8 (± 0.14)	1.64 ± 0.08	TB	This Work
$[Cu(L\text{-}tyr)(bpy)]^{+}$	0.8 (±0.10)	-----	SP	31
$[Cu(L\text{-}tyr)(5,6\text{-}dmp)]^{+}$	6.5 (±0.12)	-----	SP	31
$[Cu(L\text{-}tyr)(dpq)]^{+}$	9.8 (±0.16)	-----	SP	31
$[Cu(phen)(Pro)(H_2O)]^{+}$	3.86	0.15	SP	32
$[Cu(bpy)(Pro)(H_2O)]^{+}$	4.6	0.11	SP	32
$[Cu(phen)(\ L\text{-}tyr)(H_2O)]^{+}$	3.75	0.39	SP	33
$[Cu(phen)(L\text{-}phe)(BPEI)]^{+}$	672	0.193	SP	34

TB = Trigonal bipyramid; SP = Square pyramidal; bpy = 2,2′-Bipyridine; phen = 1,10-phenanthroline; 5,6-dmp = 5,6-dimethyl-1,10-phenanthroline; dpq = dipyridoquinoxaline; phe = phenyl alanine; BPEI = branched polyethyleneimine; Pro = Proline

complete or partially stack into the DNA grooves.[11] In comparison to other copper(II) complexes, even those with amino acids in their structure (Table 1), the value of K_b calculated for $[Cu^{II}(2CP\text{-}Bz\text{-}SMe)]^{2+}$ is relatively high. This high value can be associated to the phenanthroline rings which facilitate the interaction with the base-pairs of DNA through π-stacking. Further studies on the interaction of $[Cu(2CP\text{-}Bz\text{-}SMe)]^{2+}$ with DNA were performed by fluorescence spectroscopy using ethidium bromide (EB) as probe. EB is widely known to intercalate into the double helix of DNA through electrostatic binding forming an adduct that strongly enhances the EB emission at 590 nm.[37] Thus, competitive displacement of EB by a stronger binder can be measured by following the decay of EB emission.[37,38] Additions of $[Cu(2CP\text{-}Bz\text{-}SMe)]^{2+}$ to solutions of ct-DNA incubated with EB resulted in hypochromism of the emission band at 590 nm, as shown in Fig. 2 (C), indicating the displacement of EB while the complex intercalates into the same domains. The Stern-Volmer constant (K_{SV}), which gives the magnitude of the interaction strength, was calculated as 1.64 (±0.08) from the slope of the plot of the ratio of the EB intensities against the concentration of the complex, Fig. 2 (D), according to Equation 2. Such K_{SV} value is one order of magnitude greater than the similar copper complexes displayed in Table 1.

Several aspects should be considered to explain the interaction of the compounds displayed in Table 1 with DNA where $[Cu(phen)(L\text{-}phe)(BPEI)]^{+}$ shows the highest binding constant. This higher value was ascribed to both the positive charge and large number of subunits of $[Cu(phen)(L\text{-}phe)]^{+}$ that compose the polymeric chain of $[Cu(phen)(L\text{-}phe)(BPEI)]^{+}$.[34] On the other hand, the K_{SV} value is 8.5 times lower than that calculated for $[Cu(2CP\text{-}Bz\text{-}SMe)]^{2+}$ indicating a lower interaction strength. Complexes derived from phenanthroline and bipyridine containing proline (Pro) and tyrosine (L-tyr) show K_{SV} constants one order of magnitude lower in comparison to $[Cu(2CP\text{-}Bz\text{-}SMe)]^{2+}$, despite the amino acid moieties that would enhance the biocompatibility. Besides the electrostatic arguments, the geometric conformation also matters.[39,40] Unlike the above mentioned Cu complexes, which are square pyramidal, the $[Cu(2CP\text{-}Bz\text{-}SMe)]^{2+}$ complex has a distorted trigonal bipyramidal geometry. We hypothesize such conformation may allow the phenanthroline fragments to be better accommodated into the double helix. Moreover, the aromaticity of these fragments increases the local hydrophobicity, as opposed to the amino acid moieties, thus increasing the affinity for the hydrophobic cavities of DNA.

Cytotoxic assays

The in vitro cytotoxicity profile of $[Cu(2CP\text{-}Bz\text{-}SMe)]^{2+}$ was investigated on A549 (lung adenocarcinoma), MCF-7 (hormone-dependent human breast), MDA-MB-231 (triple negative human breast) and MG-63 (bone fibroblast) by MTT assay (see experimental section for details). The percent of the cell viability was calculated by dividing the average absorbance of the cells treated with $[Cu(2CP\text{-}Bz\text{-}SMe)]^{2+}$ by that of the control. Furthermore, the percentage of cell viability versus the concentration of the complex (log scale) was plotted to determine the half maximal inhibitory concentration (IC_{50}), with their estimated error derived from the mean of 3 trials. Table 2 displays these results for $[Cu(2CP\text{-}Bz\text{-}SMe)]^{2+}$ along with those reported for cisplatin (CPPD), a clinical reference drug, and similar copper complexes for comparative purpose.

The cytotoxic assays show that $[Cu(2CP\text{-}Bz\text{-}SMe)]^{2+}$ has potent cytotoxicity in the three cell lines studied (MDA-MB-231 = 4.62 ± 0.48 μM; MCF-7= 5.2 ± 0.76 μM; A549 = 5.7 ± 0.42 μM; MG-63 = 2.88 ± 0.66 μM), with an IC_{50} lower than cisplatin. The IC_{50} values determined for $[Cu(2CP\text{-}Bz\text{-}SMe)]^{2+}$ are considerably lower than those for monometallic copper complexes derived from homo and heteroleptic phenanthroline ligands. Furthermore, the comparison of K_{SV} values made between $[Cu(2CP\text{-}Bz\text{-}SMe)]^{2+}$ and compounds containing amino acids also holds for IC_{50} in cell lines MCF-7 and A549. In comparison to [Cu(3-Clip-phen)], which has a very analogous structure and presents significant antiproliferative action towards L1210 murine leukemia cell line,[9] $[Cu(2CP\text{-}Bz\text{-}SMe)]^{2+}$ shows lower IC_{50} values for MCF-7 and A549 cell lines. Such trend is observed for the A549 cell line even with respect to $[Cu(3\text{-}Clip\text{-}phen)\text{-}(CH_2)_6\text{-}CDDetP]$ which contains a cisplatin moiety attached to the ethylenediamine unit.[41]

Plasmid pBR322 cleavage assays

We ascribe the effectiveness of $[Cu(2CP\text{-}Bz\text{-}SMe)]^{2+}$ in interacting with DNA to the synergy of its positive charge, complex geometry, presence of aromatic moieties and the ability of the complex to be reversible reduced to Cu(I) thus generating ROS. These factors act in tandem with ability of the complex to produce $OH^{\bullet}$ through a Fenton-like catalytic mechanism involving the copper metal center.[45,46] To explore *in vitro* conditions, we further probed the ability of $[Cu(2CP\text{-}Bz\text{-}SMe)]^{2+}$ to produce $OH^{\bullet}$ in the presence of ascorbic acid (AA), nicotinamide adenine dinucleotide (NADH), and glutathione (GSH), which are reducing substances commonly found in the cellular medium. AA donates two electrons, preventing other substances from oxidizing and imparting it potent antioxidant properties.[47,48] NADH, besides being a cofactor for a few intracellular redox processes, presents an abnormal concentration increase in breast cancer cells.[49,50]

View Article Online
DOI: 10.1039/D1DT01358K

Table 2. IC_{50} values of copper complexes and cisplatin (CPPD) after 48 h of incubation.

Complex	MG-63	MDA-MB-231	MCF-7	A549	Ref.
CDDP*	33.0 ± 3	11.0 ± 2	13.98 ± 2.02	14.42 ± 1.45	57, 30, 58
$[Cu(2CP\text{-}Bz\text{-}SMe)]^{2+}$	2.88 ± 0.66	4.62 ± 0.48	5.20 ± 0.76	5.70 ± 0.42	This work
$[Cu(3\text{-}Clip\text{-}phen)]^{2+}$		-----	> 10	> 10	41
$[Cu(3\text{-}Clip\text{-}phen)\text{-}(CH_2)_6\text{-}CDD_{et}P]$		-----	3	> 10	41
$[Cu(3\text{-}Clip\text{-}phen)\text{-}(CH_2)_{10}\text{-}CDD_{et}P]$		-----	> 10	> 10	41
$[Cu(PYIP)_2(H_2O)]^{2+}$		26.5 ± 1.50	-----	38.2 ± 1.10	42
$[Cu(CN\text{-}PIP)_2(H_2O)]^{2+}$		40.0 ± 4.60	-----	71.8 ± 4.70	42
$[Cu(L1)(2,9\text{-}dmp)]^{2+}$		-----	11.3 ± 1.10	-----	43
$[Cu(L2)(2,9\text{-}dmp)]^{2+}$		-----	12.4 ± 1.80	-----	43
$[Cu(L3)(2,9\text{-}dmp)]^{2+}$		-----	16.1 ± 0.50	-----	43
$[Cu(L4)(2,9\text{-}dmp)]^{2+}$		-----	16.4 ± 1.20	-----	43
$[Cu(phen)_2]^{2+}$		-----	14	14	44
[Cu(Gly-Val)(phen)]		-----	18	9.5	44
[Cu(Ala-Gly)(phen)]		-----	16	9.5	44
[Cu(Phe-Ala)(phen)]		-----	13	9.9	44
[Cu(Phe-Val)(phen)]		-----	7.4	7.1	44
[Cu(Phe-Phe)(phen)]		-----	9.6	7.8	44

*Values obtained in NaCl. (L1) = diethylenetriamine; (L2) = N-methyl-N'-(pyrid-2-ylmethyl) ethylenediamine; (L3) = di(2-picolyl)amine; (L4) = bis(pyrid-2-ylmethyl)-N-methylamine and (2,9-dmp) = 2,9-dimethyl-1,10-phenanthroline. $CDD_{et}P$ = *cis*-dichloro-diethylamino-platinate.

GSH is synthesized in the cytosol and plays a fundamental role protecting cells from oxidative damage, maintaining redox homeostasis.[51] Increases in GSH levels on cancer cells are ascribed to an increased production of γ-glutamylcysteine synthetase, a rate-limiting enzyme involved in GSH biosynthesis. biosynthesis.[52,53] Indeed, concentration increase of GSH is one of the reasons of cancer cell resistance to chemotherapy with cisplatin.[54,55]

For these reasons, we explored the effect of the $[Cu(2CP\text{-}Bz\text{-}SMe)]^{2+}$ complex in nuclease assays in the presence of NADH, GHS, and AA at concentrations relevant to normal and cancer cells.[51,56] Figure 3 shows electrophoresis results obtained for the relaxation of the supercoiled circular plasmid pBR322 DNA (Form I) into nicked (Form II) and linear (Form III) in aerated aqueous medium using two different concentrations for NADH and GHS, and one for AA.

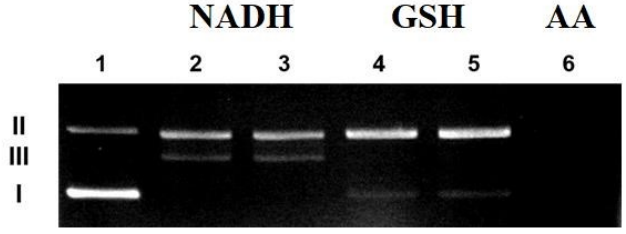

Figure 3. Nicked and cleaved plasmid pBR322 DNA by 10 µM of Cu(II)* in presence of the reducing agents NADH, GSH, and AA. **1.** DNA + Cu(II); **2.** DNA + Cu(II) + NADH 0.1 mM; **3.** DNA + Cu(II) + NADH 0.2 mM; **4.** DNA + Cu(II) + GSH 1.5 mM; **5.** DNA + Cu(II) + GSH 4 mM; **6.** DNA + Cu(II) + AA 0.1 mM. *Cu(II) = $[Cu(2CP\text{-}Bz\text{-}SMe)]^{2+}$.

As previously reported,[18] no nuclease activity was observed for $[Cu(2CP\text{-}Bz\text{-}SMe)]^{2+}$ in the absence of reducing agents (lane 1). For both concentrations of NADH (lanes 2 and 3) two bands were observed, with the more intense one corresponding to the nicked DNA (Form II). For GSH, the nuclease activity led to the nicked form regardless the concentration (lanes 4 and 5), while a complete degradation was observed in presence of AA 0.1 mM (lane 1). Therefore, all nuclease assays in presence of the biological reducing agents showed the $[Cu(2CP\text{-}Bz\text{-}SMe)]^{2+}$ complex is effective in partially or completely degrading DNA.

ESR measurements

The generation of $OH^{\bullet}$ by $[Cu(2CP\text{-}Bz\text{-}SMe)]^{2+}$ was previously reported by Romo et al[18] using N-tert-butyl-α-phenylnitrone (PBN) as spin trap. In this work, ESR spectra were also acquired for this complex in solution (Figure 4) containing the reducing agents used in the nuclease activity assays (AA, GSH and NADH) along with 5,5-Dimethyl-1-pyrroline-N-oxide (DMPO) as spin trap.

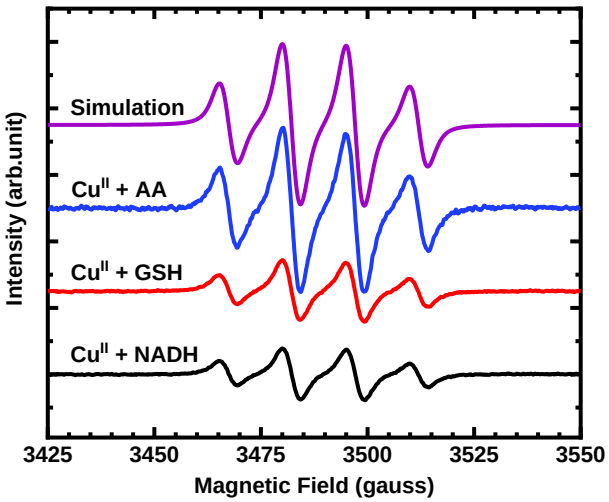

Figure 4. ESR spectra of $[Cu(2CP\text{-}Bz\text{-}SMe)]^{2+}$ complex in aqueous solution containing AA (blue line), GSH (red line), and NADH (black line). Spectral simulations were made with the EasySpin program.[60] DMPO-OH adduct was identified (g = 2.00575, A^N = 15.0 G and A^H = 14.9 G).

Hyperfine couplings for the DMPO-OH adduct are consistent with OH• generation. The values of AN = 15.0 G and AH = 14.9 G are in

accordance with previous data reported for the same adduct in water,[61] proving that the nuclease activity observed for [Cu(2CP-Bz-SMe)]$^{2+}$ depends on the generation of OH$^{\bullet}$. In comparison to the results observed in the presence of GSH and NADH, a higher intensity of the DMPO-OH adduct was observed for AA, indicating a greater generation of OH$^{\bullet}$. Accordingly, DNA is fully degraded in presence of AA whereas NADH and GSH promote the nicked and linear forms, respectively (see Figure 3).

PCR inhibition

To evaluate if [Cu(2CP-Bz-SMe)]$^{2+}$ can interfere with DNA amplification, polymerase chain reactions (PCR) experiments were performed using a bacterial DNA as template and two primers that amplify a 1.3 kbp region together with DNA polymerase and deoxynucleotides using different concentrations of copper complex and a control reaction without complex. The reaction products were followed by agarose gel electrophoresis and the images are illustrated in Figure 5.

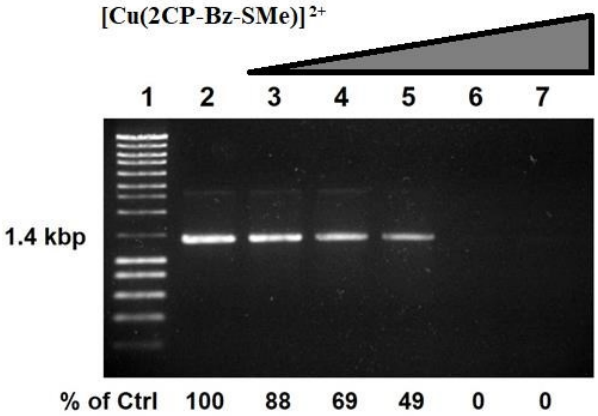

Figure 5. PCR inhibition assays with *Cu(II), using 0.2U of DNA polymerase. **1.** Oligonucleotide ladder; **2.** control without Cu(II) ; **3.** 1µM Cu(II) **4.** 2µM Cu(II); **5.** 3µM Cu(II); **6.** 4µM Cu(II) **7.** 5µM Cu(II); *Cu(II) = [Cu(2CP-Bz-SMe)]$^{2+}$. Band intensities are reported as percentage of the intensity of the control band.

The copper complex inhibited the DNA amplification even at the lowest concentration used, 1 µM (lane 3). Increasing the concentration to 3 µM (lane 5) led to an intensity decrease of 51% in respect to the control (lane 2) while a complete blockage was observed in line 6 at 4 µM of [Cu(2CP-Bz-SMe)]$^{2+}$. We hypothesize the inhibition of the DNA polymerase replication in PCR by this compound is due to its intercalation into the DNA by a π-stacking interaction between the aromatic rings of the 2CP-Bz-SMe moiety with the nitrogenous bases of DNA, as supported by the competition study with EB (Figure 2). The competition of the DNA polymerase with [Cu(2CP-Bz-SMe)]$^{2+}$ was evaluated using the concentration of total inhibition of replication (4 µM) and varying DNA polymerase concentrations (Figure 6).

As expected, it is not possible to replicate the DNA by using 4 µM of [Cu(2CP-Bz-SMe)]$^{2+}$ (Figure 5, lane 3). However, increasing the concentration of DNA polymerase to 0.4U and 0.9 U (lanes 4 and 5) results in the re-emergence of the DNA band. A the highest concentration, a greater increase in DNA replication was observed even in comparison to the control (lane 2). These results

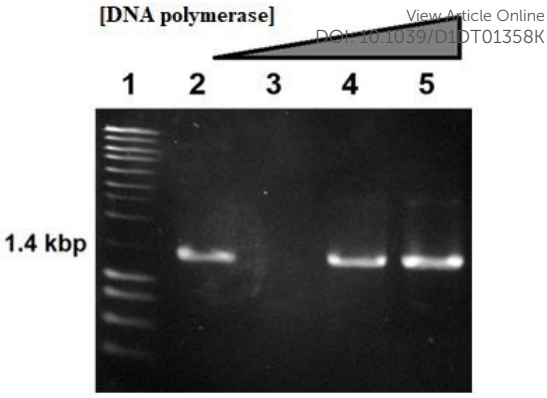

Figure 6. Effect of DNA polymerase and DNA template on the inhibition of PCR by [Cu(2CP-Bz-SMe)]$^{2+}$ (4 µM). **1.** ladders; **2.** control: no copper complex and DNA polymerase 0.2U; **3.** Cu(II) + DNA polymerase 0.2U; **4.** Cu(II) + DNA polymerase 0.4U; **5.** Cu(II) + DNA polymerase 0.9U. *Cu(II) = [Cu(2CP-Bz-SMe)]$^{2+}$.

are consistent with the fact that the copper complex and DNA polymerase are competing for the DNA binding. Thus, a higher concentration of enzyme or DNA promotes the amplification of DNA, as schematically shown in Figure 7.

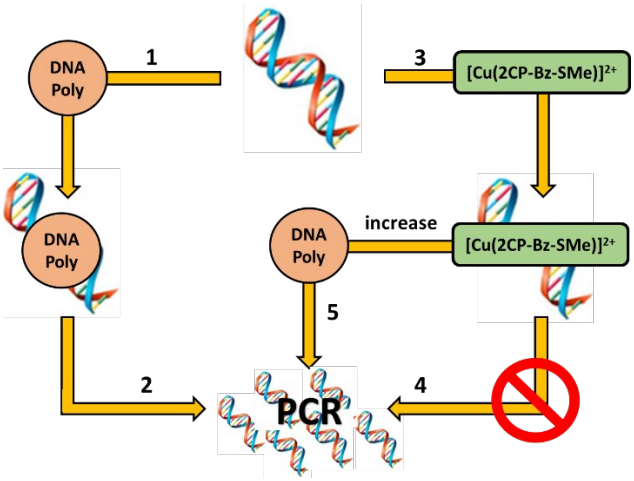

Figure 7. Proposed scheme for the competition between DNA polymerase (DNA poly) and [Cu(2CP-Bz-SMe)]$^{2+}$ for interaction with DNA. In the absence of [Cu(2CP-Bz-SMe)]$^{2+}$, the DNA polymerase interacts with DNA and proceed to amplification in the PCR reaction (steps 1 and 2). In the presence of [Cu(2CP-Bz-SMe)]$^{2+}$, the π-stacking interactions between the aromatic rings of 2CP-Bz-SMe with the nitrogenous bases of DNA prevent the binding and amplification of DNA by DNA Poly in the PCR reaction (steps 3 and 4). Increasing the amount of DNA poly, the enzyme that competes with [Cu(2CP-Bz-SMe)]$^{2+}$ for the DNA binding can, again, amplify the DNA fragment in the PCR reaction (steps 5 and 2).

Conclusions

We demonstrated the efficient DNA binding and polymerase inhibition of $[Cu(2CP\text{-}Bz\text{-}SMe)]^{2+}$. The NMR of ligand and mass spectra of $[Cu(2C\text{-}Bz\text{-}SMe)]^{2+}$, where 2C-Bz-SMe = 1,3-bis(1,10-phenanthrolin-2-yloxy)-N-(4-(methylthio)benzylidene)propan-2-amine, confirmed this compound was successfully obtained by following the synthetic procedure described in the literature. Binding studies of the complex with Calf-Thymus DNA (ct-DNA) were performed by absorption titration and competitive fluorescence assays using ethidium bromide (EB) as a probe to determine, the binding (K_b) and Stern-Volmer (K_{SV}) constants, respectively. Additions of ct-DNA to the solution of $[Cu(2CP\text{-}Bz\text{-}SMe)]_{2+}$ resulted in hypochromism of the intraligand bands indicating that the complex interacts with DNA with a binding constant of $5.8 \pm 0.14 \times 10^4$. The observed decrease of the EB emission at 590 nm during the additions of $[Cu(2CP\text{-}Bz\text{-}SMe)]^{2+}$ to solutions of ct-DNA incubated with EB indicated the displacement of EB while the complex intercalates into the same domains resulting in a K_{SV} value of 1.64 (±0.08). Polymerase chain reactions (PCR) experiments indicated the complex inhibits the DNA amplification even at the lowest concentration used, 1 μM. Such behavior was ascribed to the intercalation ability in the DNA that occurs, mainly, by π-stacking interaction between the aromatic rings of the 2CP-Bz-SMe moiety with the nitrogenous bases of DNA, reinforcing the evidence obtained by the competition study with EB. Besides the intercalation ability, previous works showed the $[Cu(2CP\text{-}Bz\text{-}SMe)]^{2+}$ complex produces hydroxyl radical ($OH^{\bullet}$) in aqueous aerated medium. To mimic in vivo conditions, we evaluated the ability of $[Cu(2CP\text{-}Bz\text{-}SMe)]^{2+}$ to produce $OH^{\bullet}$ in the presence of ascorbic acid, nicotinamide adenine dinucleotide, and glutathione. While no nuclease activity was observed for $[Cu(2CP\text{-}Bz\text{-}SMe)]^{2+}$ in the absence of reducing agents, the addition of the biological reducing agents resulted in partial or complete DNA degradation. The $[Cu(2CP\text{-}Bz\text{-}SMe)]^{2+}$ complex showed cytotoxicity against the following human cancer cells lines A549, MCF-7, MDA-MB-231 and MG-63 with half maximal inhibitory concentration (IC_{50}) values of 4.62 ± 0.48, 5.20 ± 0.76 and 5.70 ± 0.42, 2.88 ± 0.66 μM respectively. In a whole scenario, the results show that the phenanthroline derivative coordinated to the copper metal center is capable not only of facilitating intercalation into the DNA minor grooves, but also to allow oxidation changes without ligand dissociation. The oxidation state changes, in turn, produce $OH^{\bullet}$ that results in DNA cleavage. These features, operating in tandem, might explain the low values of IC_{50} obtained for the A549, MCF-7, MDA-MB-231 and MG-63 cancer cells lines, which are promising when compared to cisplatin, a clinical reference drug.

Author Contributions

A. I. B. Romo and I. C. N. Diógenes designed the experiments and wrote the manuscript. M. P. Carepo and P. Levin run the PCR experiments, D. E. Díaz, L. F. Bezerra, and A. I. B. Romo carried out the syntheses and characterizations of the ligand and the cupric complex. O. R. Nascimento conducted the measurement, analysis and interpretation of ESR, L. Lemus and I. E. Leon conducted the DNA cleavage and biological assays, respectively. J. Rodriguez-López interpreted the data and revised the manuscript.

Conflicts of interest

There are no conflicts to declare.

Acknowledgements

This work was supported by UNLP (X041), CONICET (PIP 0340), and ANPCyT (PICT 2016-1574), from Argentina, and Coordenação de Aperfeiçoamento de Pessoal de Nível Superior - Brasil (CAPES) - Finance Code 001 (PROEX 23038.000509/2020-82). I. C. N. Diógenes (#311274/2020-0), A. I. B. Romo (# 72170429), P. Levin (#21160546), and (M. S. P. Carepo (UID/QUI/50006/2019) are thankful to CNPq, CONICYT, ANID, and FCT/MCTES for the grants.

References

1 N. Ma, A. van der Vaart, J. Am. Chem. Soc. 2016, **138**, 9951-9958.
2 M.W. Szulik, M.W. Voehler, M. Ganguly, B. Gold, M.P. Stone, Biochemistry 2013, **52**, 7659-7668.
3 K. Sato, K. Kawamoto, S. Shimamura, S. Ichikawa, A. Matsuda, Bioorg. Med. Chem. Lett. 2016, **26**, 5395-5398.
4 J. Jin, J. Hu, Y. Qin, J. Zhang, J.a. Zhao, L. Yue, H. Hou, New J. Chem. 2019, **43**, 19286-19297.
5 A. Hussain, M.F. AlAjmi, M.T. Rehman, S. Amir, F.M. Husain, A. Alsalme, M.A. Siddiqui, A.A. AlKhedhairy, R.A. Khan, Sci. Rep. 2019, **9**, 5237.
6 K.E. Prosser, S.W. Chang, F. Saraci, P.H. Le, C.J. Walsby, J. Inorg. Biochem. 2017, **16**, 789-99.
7 M. Nagai, N.H. Vo, L. Shin Ogawa, D. Chimmanamada, T. Inoue, J. Chu, B.C. Beaudette-Zlatanova, R. Lu, R.K. Blackman, J. Barsoum, K. Koya, Y. Wada, Free Radicals Biol. Med. 2012, **52**, 2142-2150.
8 M. Pitié, B. Donnadieu, B. Meunier, Inorg. Chem. 1998, **37**, 3486-3489.
9 M. Pitié, A. Croisy, D. Carrez, C. Boldron, B. Meunier, ChemBioChem 2005, **6**, 686-691.
10 M. Pitié, B. Meunier, Bioconjugate Chem. 1998, **9**, 604-611.
11 A. Robertazzi, A. Magistrato, P. de Hoog, P. Carloni, J. Reedijk, Inorg. Chem. 2007, **46**, 5873-5881.
12 J.-M. Lehn, Science, 2002, **295**, 2400-2403.
13 D.H. Jara, L. Lemus, L. Farias, E. Freire, R. Baggio, J. Guerrero, Eur. J. Inorg. Chem. ,2012, **10**, 1579-1583.
14 S. Kim, J.W. Ginsbach, J.Y. Lee, R.L. Peterson, J.J. Liu, M.A. Siegler, A.A. Sarjeant, E.I. Solomon, K.D. Karlin, J. Am. Chem. Soc. 2015, **137**, 2867-2874.
15 P.J. Jansson, P.C. Sharpe, P.V. Bernhardt, D.R. Richardson, J. Med. Chem. 2010, **53**, 5759-5769.
16 S. Kim, J.Y. Lee, R.E. Cowley, J.W. Ginsbach, M.A. Siegler, E.I. Solomon, K.D. Karlin, J. Am. Chem. Soc. 2015, **137**, 2796-2799.
17 M.A.S. Silva, A.I.B. Romo, D.S. Abreu, M.S.P. Carepo, L. Lemus, M. Jafelicci, T.F. Paulo, O.R. Nascimento, E. Vargas, J.C. Denardin, I.C.N. Diógenes, J. Inorg. Biochem. 2018, **186**, 294-300.
18 A.I.B. Romo, D.S. Abreu, T. de F. Paulo, M.S.P. Carepo, E.H.S. Sousa, L. Lemus, C. Aliaga, A.A. Batista, O.R. Nascimento, H.D. Abruña, I.C.N. Diógenes, Chem. - Eur. J. 2016, **22**, 10081-10089.
19 H.-C. Liang, K.D. Karlin, R. Dyson, S. Kaderli, B. Jung, A.D. Zuberbühler, Inorg. Chem. 2000, **39**, 5884-5894.

20 T. Tano, K. Mieda, H. Sugimoto, T. Ogura, S. Itoh, Dalton Trans. 2014, **43**, 4871-4877.
21 S.T. Prigge, B.A. Eipper, R.E. Mains, L.M. Amzel, Science, 2004, **304**, 864-867.
22 P. Chen, E.I. Solomon, J. Am. Chem. Soc. 2004, **126**, 4991-5000.
23 Z. Tyeklar, K.D. Karlin, Acc. Chem. Res. 1989, **22**, 241-248.
24 A.I.B. Romo, V.S. Dibo, D.S. Abreu, M.S.P. Carepo, A.C. Neira, I. Castillo, L. Lemus, O.R. Nascimento, P.V. Bernhardt, E.H.S. Sousa, I.C.N. Diógenes, Dalton Trans. 2019, **48**, 14128–14137.
25 J. Marmur, J. Mol. Biol. 1961, **3**, 208-IN201.
26 M.E. Reichmann, S.A. Rice, C.A. Thomas, P. Doty, J. Am. Chem. Soc. 1954, **76**, 3047-3053.
27 H.J. Li, D.M. Crothers J. Mol. Biol. 1969, **39**, 461-477.
28 A. Wolfe, G.H. Shimer, T. Meehan, Biochemistry, 1987, **26**, 6392-6396.
29 O. Stern, M. Volmer, Z. Phys. 1919, **20**, 6.
30 W. Villarreal, L. Colina-Vegas, G. Visbal, O. Corona, R.S. Corrêa, J. Ellena, M.R. Cominetti, A.A. Batista, M. Navarro, Inorg. Chem. 2017, **56**, 3781-3793.
31 S. Ramakrishnan, V. Rajendiran, M. Palaniandavar, V.S. Periasamy, B.S. Srinag, H. Krishnamurthy, M.A. Akbarsha, Inorg. Chem. 2009, **48**, 1309-1322.
32 P.R. Reddy, N. Raju, P. Manjula, K.V. Reddy, Chem. Biodivers, 2007, **4**, 1565-1577.
33 P.R. Reddy, P. Manjula, Chem Biodivers, 2009, **6**, 71-78.
34 R.S. Kumar, S. Arunachalam, Eur. J. Med. Chem. 2009, **44**, 1878-1883.
35 R.A. Rader, D.R. McMillin, M.T. Buckner, T.G. Matthews, D.J. Casadonte, R.K. Lengel, S.B. Whittaker, L.M. Darmon, F.E. Lytle, J. Am. Chem. Soc. 1981, **103**, 5906-5912.
36 A. Kunishita, M. Kubo, H. Ishimaru, T. Ogura, H. Sugimoto, S. Itoh, Inorg. Chem. 2008, **47**, 12032-12039.
37 J.B. LePecq, C. Paoletti, J. Mol. Biol. 1967, **27**, 87-106.
38 H.M. Berman, P.R. Young, Annu. Rev. Biophys. Bioeng. 1981, **10**, 87-114.
39 G. Barone, A. Terenzi, A. Lauria, A.M. Almerico, J.M. Leal, N. Busto, B. García, Coord. Chem. Rev. 2013, **257**, 2848-2862.
40 M. Iqbal, S. Ali, A. Haider, N. Khalid, Iran. J. Sci. Technol., Trans. A: Sci. 2018, **42**,1859-1871.
41 P. de Hoog, C. Boldron, P. Gamez, K. Sliedregt-Bol, I. Roland, M. Pitié, R. Kiss, B. Meunier, J. Reedijk, J. Med. Chem. 2007, **50**, 3148-3152.
42 P. Nagababu, A.K. Barui, B. Thulasiram, C.S. Devi, S. Satyanarayana, C.R. Patra, B. Sreedhar, J. Med. Chem. 2015, **58**, 5226-5241.
43 M. Ganeshpandian, S. Ramakrishnan, M. Palaniandavar, E. Suresh, A. Riyasdeen, M.A. Akbarsha, J. Inorg. Biochem. 2014, **140**, 202-212.
44 S. Iglesias, N. Alvarez, M.H. Torre, E. Kremer, J. Ellena, R.R. Ribeiro, R.P. Barroso, A.J. Costa-Filho, M.G. Kramer, G. Facchin, J. Inorg. Biochem. 2014, **139**, 117-123.
45 G.R.A. Johnson, N.B. Nazhat, Journal of the American Chemical Society, 1987, **109**, 1990-1994.
46 S.E. Hardwick, G.R.A. Johnson, N.B. Nazhat, Int. J. Radiat. Biol. 1988, **53**, 997-997.
47 W.M. Cort, Ascorbic Acid: Chemistry, Metabolism, and Uses, Advances in Chemistry, AMERICAN CHEMICAL SOCIETY, 1982, **200**, 533-550.
48 A. Akbari, G. Jelodar, S. Nazifi, J. Sajedianfard, J Res Med Sci. 2016, **18**, e4037.
49 A. Uppal, P.K. Gupta, Biotechnol. Appl. Biochem. 2003, **37**, 45-50.
50 H. Huang, S. Banerjee, K. Qiu, P. Zhang, O. Blacque, T. Malcomson, M.J. Paterson, G.J. Clarkson, M. Staniforth, V.G. Stavros, G. Gasser, H. Chao, P.J. Sadler, Nat. Chem. 2019, **11**,1041-1048.
51 H.J. Forman, H. Zhang, A. Rinna, Mol. Aspects Med. 2009, **30**, 1-12.
52 A.K. Godwin, A. Meister, P.J. O'Dwyer, C.S. Huang, T.C. Hamilton, M.E. Anderson, Proc. Natl. Acad. Sci. U. S. A. 1992, **89**, 3070-3074.
53 K. Hamaguchi, A.K. Godwin, M. Yakushiji, P.J. O'Dwyer, R.F. Ozols, T.C. Hamilton, Cancer Res. 1993, **53**, 5225-5232.
54 S. Goto, T. Iida, S. Cho, M. Oka, S. Kohno, T. Kondo, Free Radical Res. 1999, **31**, 549-558.
55 M. Sakamoto, A. Kondo, K. Kawasaki, T. Goto, H. Sakamoto, K. Miyake, Y. Koyamatsu, T. Akiya, H. Iwabuchi, T. Muroya, K. Ochiai, T. Tanaka, Y. Kikuchi, Y. Tenjin, Hum. Cell. 2001, **14**, 305-315.
56 A. Gölcü, H. Muslu, D. Kılıçaslan, M. Çeşme, Ö. Eren, F. Ataş, İ. Demirtaş, J. Mol. Struc. 2016, **1119**, 96-109.
57 M. Capper, A. Enriquez-Garcia, B. Lai, B. Wang, B. Gelfand, C. Shemanko, F. Jalilehvand. Dalton Trans., 2021, **50**, 5968–5977.
58 A. Matesanz, E. Jimenez-Faraco, M. C. Ruiz, L. M. Balsa, C. Navarro-Ranninger, I. E. León, A. G. Quiroga, Inorg. Chem. Front., 2018, **5**, 73-83.
59 S. Stoll, A. Schweiger, J. Magn. Reson. 2006, **178**, 42–55.
60 E. MAKINO, T. HAGIWARA, A. MURAKAMI. Radiat. Phys. Chem. 1991, **37**, No. 5/6, pp. 657-665.